0031-3998/11/6906-0561
PEDIATRIC RESEARCH

Vol. 69, No. 6, 2011
Printed in U.S.A.

Diffusion Tensor Imaging in Preterm Infants With Punctate White Matter Lesions

LAURA BASSI, ANDREW CHEW, NAZAKAT MERCHANT, GARETH BALL, LUCA RAMENGHI, JAMES BOARDMAN, JOANNA M. ALLSOP, VALENTINA DORIA, TOMOKI ARICHI, FABIO MOSCA, A. DAVID EDWARDS, FRANCES M. COWAN, MARY A. RUTHERFORD, AND SERENA J. COUNSELL

Department of Maternal and Paediatric Sciences [L.B., L.R., F.M.], Fondazione IRCCS a Grande Ospedale Maggiore Policlinico, University of Milan, Milano 20122, Italy; Centre for the Developing Brain [A.C., N.M., G.B., J.B., J.M.A., V.D., T.A., A.D.E., F.M.C., M.A.R., S.J.C.], Imperial College and MRC Clinical Sciences Centre, Hammersmith Hospital, London W12 0HS, United Kingdom

ABSTRACT: Our aim was to compare white matter (WM) microstructure in preterm infants with and without punctate WM lesions on MRI using tract-based spatial statistics (TBSS) and probabilistic tractography. We studied 23 preterm infants with punctate lesions, median GA at birth 30 (25–35) wk, and 23 GA- and sex-matched preterm controls. TBSS and tractography were performed to assess differences in fractional anisotropy (FA) between the two groups at term equivalent age. The impact of lesion load was assessed by performing linear regression analysis of the number of lesions on term MRI *versus* FA in the corticospinal tracts in the punctate lesions group. FA values were significantly lower in the posterior limb of the internal capsule, cerebral peduncles, decussation of the superior cerebellar peduncles, superior cerebellar peduncles, and pontine crossing tract in the punctate lesions group. There was a significant negative correlation between lesion load at term and FA in the corticospinal tracts ($p = 0.03$, adjusted $r^2 = 0.467$). In conclusion, punctate lesions are associated with altered microstructure in the WM fibers of the corticospinal tract at term equivalent age. **(*Pediatr Res* 69: 561–566, 2011)**

MRI is increasingly being used to investigate brain development and pathology in infants who are born preterm. In addition to the major destructive white matter (WM) lesions, such as periventricular leukomalacia (PVL) and hemorrhagic periventricular infarction (HPI), that are observed on ultrasound, MRI studies have identified multiple punctate lesions in the WM in this group of infants. These lesions are observed as high signal intensity on T1-weighted imaging and low signal on T2-weighted imaging. Their distribution is widespread throughout the WM, and these lesions have been observed in the centrum semiovale (CSO), the corona radiata, the posterior periventricular WM (PPWM), the optic radiation, and, occasionally, in the frontal WM (1–4). They are quite common, being observed in 22% of infants in an unselected consecutive cohort and are more frequently observed in the preterm period than at term equivalent age (2).

Diffusion tensor imaging (DTI) is an MRI technique that utilizes the Brownian motion of water in tissue (5). Within WM water diffuses preferentially along axons and is restricted perpendicular to axons (6). Quantitative measures derived from DTI, such as fractional anisotropy (FA), characterize the directional preference of diffusion and provide nonsubjective measures that reflect tissue microstructure (7). In diffusion tractography, it is assumed that the principal direction of diffusion in each imaging voxel is coincident with the underlying dominant fiber direction. Tractography generates 3D representations of WM tracts by following this principal diffusion direction on a voxel by voxel basis. DTI studies have previously demonstrated differences in WM microstructure between preterm infants and term controls (8–11), and between preterm infants with diffuse or focal lesions and those with no evidence of abnormality on MRI (12,13).

Tract-based spatial statistics (TBSS) is a recently developed tool for analyzing DTI data that allows objective voxel-wise analysis free from the limitations of standard voxel-based statistical analyses, such as image registration and smoothing (14). However, TBSS examines only the center of major WM tracts and does not assess the whole extent of the tract. Probabilistic tractography is able to delineate fiber bundles in regions of low anisotropy (15), such as the more peripheral sections of tracts in the unmyelinated WM of the neonatal brain (16). Combining these two diffusion analysis techniques enables the whole brain to be surveyed in a nonsubjective fashion using TBSS and a more extensive assessment of predefined tracts to be performed using tractography.

Previous studies suggest that punctate lesions may be associated with delayed brain maturation (3). To date, however, there have been no DTI studies assessing objectively the WM in infants with punctate lesions. The aim of this study was to compare WM microstructure in preterm infants with and without punctate lesions on MRI using TBSS and probabilistic tractography at term equivalent age.

Received October 5, 2010; accepted January 4, 2011.

Correspondence: Serena J. Counsell, Ph.D., Imperial College London, Hammersmith Hospital, Robert Steiner MR Unit, Imaging Sciences Department, DuCane Road, London W12 0HS, United Kingdom; e-mail: serena.counsell@imperial.ac.uk

Supported by the Medical Research Council (UK) and Imperial College Healthcare Comprehensive Biomedical Research Centre Funding Scheme.

Abbreviations: CSO, centrum semiovale; **DEHSI,** diffuse excessive high signal intensity; **DTI,** diffusion tensor imaging; **FA,** fractional anisotropy; **GLH,** germinal layer hemorrhage; **PLIC,** posterior limb of the internal capsule; **PVL,** periventricular leukomalacia; **PPWM,** posterior periventricular white matter; **PMA,** postmenstrual age; **SLF,** superior longitudinal fasciculus; **TBSS,** tract-based spatial statistics; **WM,** white matter

METHODS

This study was approved by the Hammersmith and Queen Charlotte's and Chelsea Hospitals Research Ethics Committee and written parental consent was obtained before scanning.

Subjects. Infants with major destructive WM lesions such as cystic PVL or HPI were excluded from the study group. Twenty-three preterm infants (born at <36 wk GA) who underwent MRI and DTI between September 2006 and January 2009 had evidence of focal punctate lesions on MRI. For each infant with punctate lesions, we selected the next preterm infant of the same sex to undergo MRI and DTI at term equivalent age and who had also had an MRI scan in the early neonatal period. The images obtained in the preterm period were assessed to ensure these infants had no evidence of punctate lesions or other lesions on their early scan. These infants formed our preterm "control" group.

The median (range) GA at birth for the 23 infants with punctate lesions was 30 (25^{+3}–35^{+2}) wk and their median birthweight was 1.25 (0.86–2.50) kg. The median GA at birth for the 23 "control" infants was 30 (25^{+1} – 35^{+1}) wk and their median birthweight was 1.32 (0.69–2.17) kg. Thirteen infants were male in both groups. Clinical details for the infants are described in Table 1.

Imaging. MRI was performed on a Philips 3-T system (Philips Medical Systems, Netherlands). 3D MPRAGE imaging and T2-weighted fast spin echo were obtained before DTI. Single-shot echo planar imaging DTI was acquired in 15 noncollinear directions as described previously (8).

All examinations were supervised by a pediatrician experienced in MRI procedures. In the early neonatal period, infants were scanned after a feed. At term equivalent age, infants were scanned after sedation with oral chloral hydrate (25–50 mg/kg). Pulse oximetry, temperature, and electrocardiograph monitoring were measured throughout the MRI examination. Ear protection was used for each infant, comprising both earplugs individually molded from a silicone-based putty (President Putty; Coltene/Whaledent, Mahwah, NJ) placed in the external ear and neonatal earmuffs (Natus MiniMuffs; Natus Medical Inc., San Carlos, CA).

Data analysis. All data analysis was performed using tools included in FSL (Functional MRI of the brain software library) (17) and FA maps were generated as described previously (8).

TBSS. Voxel-wise preprocessing of the FA data acquired at term equivalent age was carried out using TBSS (14) by using an optimized protocol that we have modified to improve reliability for neonatal DTI analysis (18). Two linear registration steps were performed before nonlinear registration [6 degrees of freedom (DOF) and 12 DOF] to register every subject's FA map to each other. We selected the target with minimum mean warp displacement score as our chosen target. Each infant's FA map was aligned in the target space and an average FA map was created, that is the mean FA map. A second set of registrations was performed to register every individual FA map to the mean FA map. The aligned images were then used to create another mean FA map and a mean FA skeleton, which represented the centers of all tracts common to the group. This was thresholded to FA ≥ 0.15 to include the major WM pathways but exclude peripheral tracts where there was a significant intersubject variability and/or partial volume effects with gray matter. Each subject's aligned FA data were then projected onto this skeleton.

Table 1. *Clinical characteristics of the infants*

	Punctate lesion group	Control group	*p*
GA at birth, median (range), wk	30 (25^{+3}–35^{+2})	30 (25^{+1}–35^{+1})	0.93
Birth weight, median (range), kg	1.25 (0.86–2.50)	1.32 (0.69–2.17)	0.75
Antenatal steroids	$n = 19$	$n = 18$	0.72
Days requiring ventilation, median (range)	0 (0–10)	0 (0–8)	0.69
Days requiring nCPAP, median (range)	8 (0–59)	18 (0–49)	0.76
Chronic lung disease*	$n = 5$	$n = 4$	0.72
Culture positive sepsis	$n = 3$	$n = 2$	0.65
PDA	$n = 4$ (none required treatment)	$n = 3$ (none required treatment)	0.70
IUGR (<10th centile)	3	3	0.99

* Defined as requiring supplemental oxygen at 36 wk PMA.

Voxel-wise cross-subject statistics was performed to assess differences in FA between the two groups of infants, corrected for GA at birth and postmenstrual age (PMA) at scan. The results were corrected for multiple comparisons by controlling family-wise error rate after threshold-free cluster enhancement (TFCE).

Probabilistic tractography. Seed masks and waypoint masks were generated on color-coded FA maps.

A seed mask was drawn around the cerebral peduncle (20 voxels). Waypoint masks were drawn around the posterior limb of the internal capsule (PLIC) (21 voxels) and the central sulcus encompassing the precentral and postcentral gyrus.

The parietooccipital sulcus was identified in the parasagittal plane and the coronal plane at the most posterior edge of the sulcus was selected (19). Two seed masks of 9 × 12 voxels (width × height) were placed in the coronal plane with their medial border 1 voxel medial to the midline. The lower edge of the mask was in line with the lower edge of the corpus callosum.

Seed masks (9 voxels) were positioned in the WM lateral to the lateral geniculate nucleus as described previously (16).

Superior longitudinal fasciculus (SLF) can be identified as a triangular-shaped green tract on the color-coded FA map on a coronal slice at the level of the PLIC. A seed mask was positioned to encapsulate the SLF. A waypoint mask was drawn around the SLF on a coronal slice at the level of the splenium of the corpus callosum (19).

Connectivity distributions were generated from every voxel in the seed masks, and only those paths that went through the waypoint masks were retained. The tracts were normalized by the number of samples going from the seed mask through the waypoints (20). These connectivity distributions were then thresholded at 1%.

The FA data were tested for normality and found to be compatible with a normal distribution. Unpaired *t* tests showed no significant difference between the right and left hemispheres for FA values in the corticospinal tracts, optic radiations, and SLF ($p > 0.05$); therefore, the mean value was calculated from the bilateral measurements. FA values for the corticospinal tracts, forceps major, optic radiations, and SLF in the two groups of infants were compared using an unpaired *t* test.

RESULTS

The median PMA at term equivalent scan for the infants with punctate lesions was 41 ($39–43^{+2}$) wk and for the control group was 41^{+3} (39^{+1}–43^{+6}) wk. The median PMA at scan for the early neonatal scan for the punctate lesion group was 30 ($27–34^{+3}$) wk and for the control group was 30 (26^{+5}–35^{+5}) wk. Four infants in the punctate lesion group did not have an MRI scan in the preterm period.

There was no significant difference in GA at birth ($p = 0.93$), birthweight ($p = 0.75$), or PMA at term equivalent scan ($p = 0.73$) between the two groups of infants. There was no significant difference in the number of infants who received antenatal steroids, the number of days requiring ventilation or nasal-continuous positive airways pressure (nCPAP), who had chronic lung disease, who experienced culture positive sepsis, who had patent ductus arteriosus (PDA), or who had IUGR (defined as birthweight <10th centile), between the two groups (Table 1).

Punctate Lesions Group

***Early neonatal scan* (n = 19).** Three infants had ventricular dilatation (two mild and one moderate), one had bilateral germinal layer hemorrhage (GLH), and four had unilateral GLH (two right- and two left-sided). Seventeen infants had punctate lesions in the corona radiata/CSO [median number of lesions = 6 (2–36)], 13 infants had punctate lesions in the PPWM [median = 5 (1–15)], 12 infants had punctate lesions in the optic radiations [me-

dian = 4 (1–9)], and three infants had a single punctate lesion in the frontal WM. Figure 1 demonstrates punctate lesions in an infant imaged at 33 wk PMA.

Term equivalent scan. Sixteen infants had diffuse excessive high signal intensity (DEHSI), 11 had dilated ventricles (seven mild and four moderate), and three infants had an enlarged extracerebral space on conventional imaging. Myelination in the PLIC was appropriate for GA in 21 infants and was delayed and asymmetrical in one infant, and in the infant with the most extensive lesions, there was abnormal signal intensity bilaterally in the PLIC on T2-weighted imaging. Seventeen infants had punctate lesions in the corona radiata/CSO [median number of lesions = 5 (1–28)], 12 infants had punctate lesions in the PPWM [median = 4 (1–12)], eight infants had punctate lesions in the optic radiations [median = 2 (1–7)], and one infant had a single punctate lesion in the frontal WM.

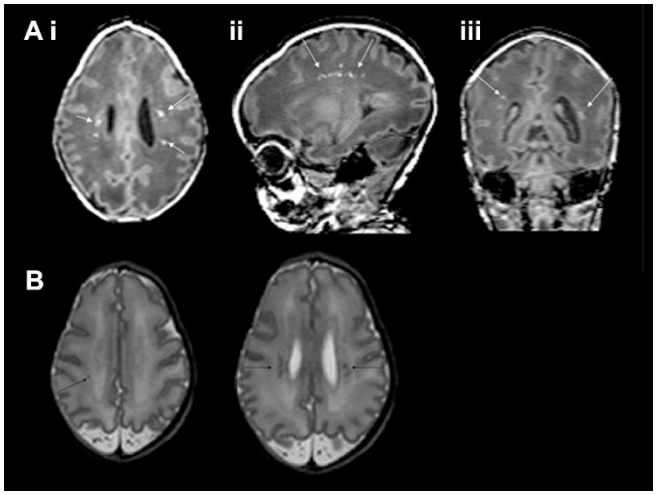

Figure 1. Images of an infant at 33 wk PMA. (*A*) T1-weighted images in the i) axial, ii) sagittal, and iii) coronal planes and (*B*) T2-weighted images in the axial plane showing multiple punctate lesions as high signal intensity on T1-weighted imaging and low signal on T2-weighted imaging (*arrows*).

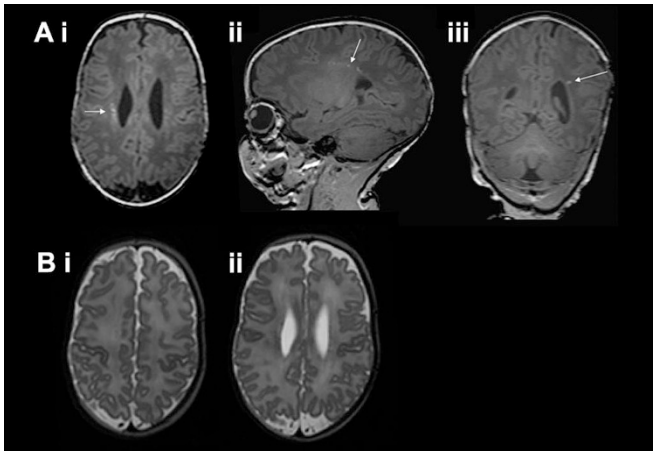

Figure 2. Images of the same infant as Figure 1 scanned at 42 wk PMA. (*A*) T1-weighted images in the i) axial, ii) sagittal, and iii) coronal planes and (*B*) T2-weighted images in the axial plane The lesions are less numerous at 42 wk PMA on T1-weighted imaging (*arrows*) and cannot be clearly identified on T2-weighted imaging.

Three infants who had punctate lesions on their early scan had no evidence of punctate lesions at term equivalent age. Figure 2 demonstrates punctate lesions in an infant imaged at 42 wk PMA.

Preterm "Control" Group

Early neonatal scan. The MRI scan was normal for GA in 13 infants, seven had mild ventricular dilatation, six had bilateral GLH, and four had unilateral GLH (two right- and two left-sided).

Term equivalent scan. Fifteen infants had DEHSI, 13 had dilated ventricles (nine mild and four moderate), and two infants had an enlarged extracerebral space. Myelination in the PLIC was appropriate for GA in all infants.

TBSS

Age at imaging. FA values throughout the WM, including the PLIC, external capsule, brain stem, cerebellum, fornix, cingulum, inferior frontooccipital fasciculus, and inferior longitudinal fasciculus (ILF) were correlated positively with PMA at scan ($p < 0.05$).

GA at birth. FA values in the corpus callosum, the PLIC, ILF, optic radiations, and left frontal WM were significantly correlated with GA at birth ($p < 0.05$).

Infants with punctate lesions* versus *preterm "control" group. FA values were significantly lower in the PLIC, cerebral peduncles, decussation of the superior cerebellar peduncles, superior cerebellar peduncles, and pontine crossing tract at term equivalent age in infants who had punctate lesions compared with those who did not after correction for GA at birth and PMA at scan and TFCE correction for multiple comparisons (Fig. 3).

Probabilistic Tractography

Mean FA values for the corticospinal tracts (Fig. 4*C*), forceps major (Fig. 4*D*), optic radiations (Fig. 4*E*), and SLF

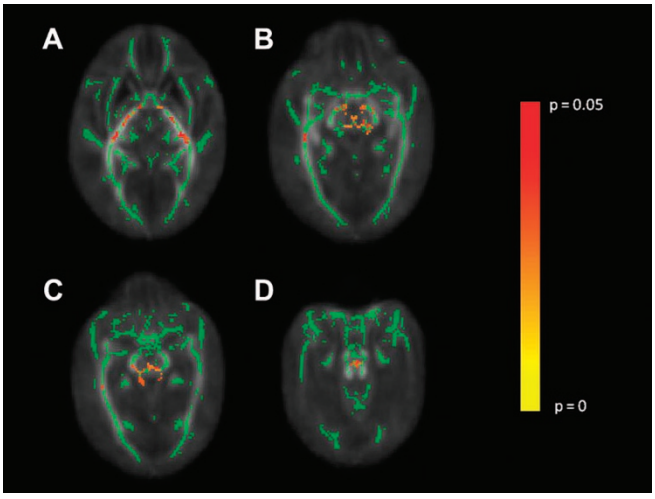

Figure 3. Voxel-wise comparison between infants with punctate lesions and those with no evidence of punctuate lesions. Voxels showing a significant reduction in FA in the punctate lesion group are shown in red-yellow and include the PLIC (*A*), cerebral peduncles and decussation of the superior cerebellar peduncles (*B*), superior cerebellar peduncles (*C*), and pontine crossing tract (*D*).

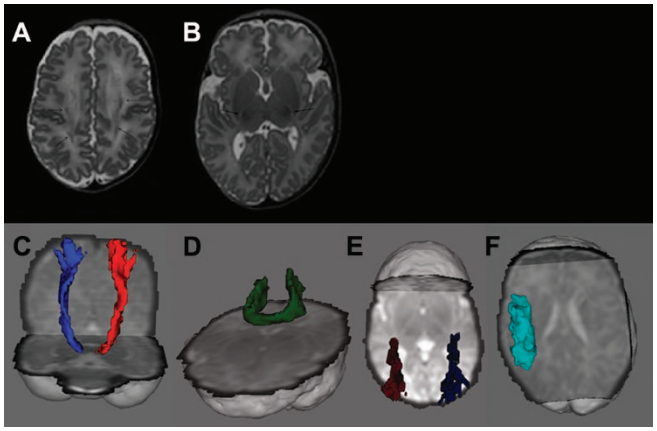

Figure 4. Images of the infant who had the most extensive lesions. (*A*) T2-weighted image at the level of the CSO. The punctate lesions are seen as low signal intensity (*arrows*). (*B*) T2-weighted imaging at the level of the basal ganglia showing abnormal high signal intensity in the PLIC (*arrows*). Probabilistic tractography of the (*C*) left (red) and right (blue) corticospinal tract, (*D*) forceps major, (*E*) optic radiations, and (*F*) SLF in this infant.

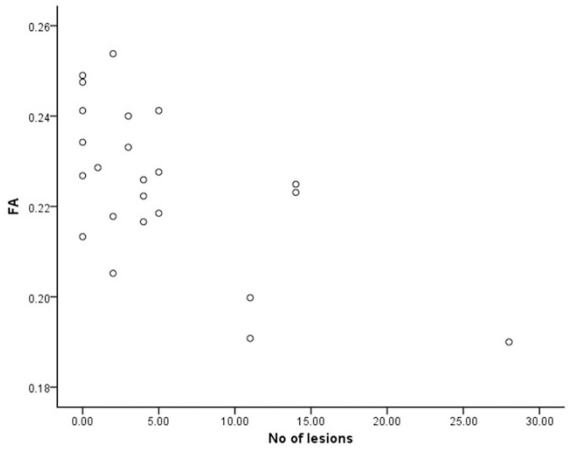

Figure 5. Graph showing FA values in the corticospinal tracts *vs* number of lesions in the corona radiata/CSO on term equivalent MRI.

Table 2. *FA values obtained by probabilistic tractography in the two groups of infants*

	Controls	Punctate lesion group	*p*
Corticospinal tracts	0.241 ± 0.017	0.225 ± 0.017	<0.01
Forceps major	0.219 ± 0.016	0.217 ± 0.012	0.61
Optic radiations	0.235 ± 0.012	0.232 ± 0.010	0.29
SLF	0.187 ± 0.085	0.179 ± 0.020	0.17

(Fig. 4*F*) for the two groups of infants are shown in Table 2. FA values in the corticospinal tracts were significantly reduced in the infants with punctate lesions compared with those without ($p < 0.01$). There were no significant differences in FA values in the forceps major, optic radiations, or SLF between the two groups.

We performed a secondary analysis to investigate the impact of lesion load at term equivalent age on FA values in the corticospinal tracts in the punctate lesions group. Linear regression analysis of FA *versus* number of lesions in the corona radiata/CSO, corrected for GA at birth and PMA at scan, demonstrated a significant negative correlation between number of lesions and FA value (Fig. 5; $p = 0.03$, adjusted $r^2 = 0.467$). This relationship failed to be significant when the infant with the most extensive lesions and abnormal signal intensity in the PLIC was removed ($p = 0.07$, adjusted $r^2 = 0.370$).

DISCUSSION

In this study, we demonstrated altered WM microstructure in the PLIC, cerebral peduncles, decussation of the superior cerebellar peduncles, superior cerebellar peduncles, and pontine crossing tracts at term equivalent age in infants who have punctate WM lesions compared with a GA- and sex-matched group of preterm infants without punctate lesions. Of interest, the distribution of reduced FA in the corticospinal tracts in the infants with punctate lesions was more widespread than the visible extent of the lesions, suggesting a diffuse injury to these tracts that is not apparent on conventional MRI.

We used an observer independent, voxel-wise approach to analyze DTI data, TBSS. Although TBSS offers a number of advantages over both qualitative image evaluation and region of interest based studies, the analysis is confined to the center of the WM tracts and may underestimate the regional extent of any abnormalities. Furthermore, because TBSS uses image registration of DTI data, it is possible that local changes in FA that are not consistent throughout the group would not be identified. Therefore, we performed probabilistic tractography to explore the WM microstructural properties along whole tracts. As the punctate lesions were largely confined to the corona radiata, CSO, PPWM, and the optic radiations, we performed tractography along the corticospinal tracts (to capture the fibers going through the corona radiata), the SLF (to capture the association fibers going through the CSO), the forceps major (to capture the fibers going through the PPWM), and in the optic radiations. Tractography demonstrated reduced FA in the punctate lesion group only in the corticospinal tracts, consistent with the TBSS findings. We also found a trend toward lesion load and reduced FA, although this relationship did not remain significant when the infant with the most extensive lesions was removed from the analysis.

Delayed brain maturation has been observed on conventional MRI in preterm infants with punctate lesions when compared with those without (3). Ramenghi *et al.* (3) described reduced myelination and cortical folding in a group of preterm infants with punctate lesions at term compared with age-matched preterm control infants. Our results of reduced FA in the PLIC in the infants with punctate lesions are consistent with their finding of delayed myelination in this structure. In addition, on visual analysis, we observed delayed myelination in the PLIC in one infant with punctate lesions and abnormal signal intensity in this structure in the infant with the most extensive lesions. Reduced FA values have been observed in the WM in preterm infants with focal lesions (9) and diffusion tractography studies have shown reduced FA in the sensory and motor pathways, corpus callosum, and PLIC in children and adolescents with PVL (21–24). In the absence of histological correlation, it is unclear whether punctate

lesions represent a milder form of cystic WM injury that is associated with preterm birth.

Similar to the findings of Cornette et al. (1) who observed many fewer lesions in the anterior WM compared with the PPWM and optic radiations, we observed punctate lesions in the frontal WM in only three infants on their early neonatal scan and these were no longer apparent at term equivalent age in two of these infants. Indeed, in this study, we observed fewer lesions at term equivalent age than we did in the preterm period in all of the infants. This is consistent with our earlier findings in a consecutive cohort of infants born at <30 wk GA who underwent MRI in the early neonatal period and at term equivalent age. In our previous study, we observed punctate lesions in 22% ($n = 26$) of infants, the median number of lesions per infant was 2 (range, 1–9), and these lesions were identifiable in only five infants at term equivalent age (2).

The etiology of punctate WM lesions is not known. It is unlikely that they represent hemorrhage as they are often less clearly seen on T2-weighted imaging than on T1-weighted imaging. It is possible that these lesions represent heterogenous pathology and susceptibility weighted imaging may prove useful in differentiating hemorrhagic from nonhemorrhagic lesions in future studies. In an isolated postmortem case, we found that areas of punctate lesions on imaging represented regions of activated microglia (25). The two groups of preterm infants in this study had comparable numbers of infants with DEHSI, ventricular dilatation, and increased extracerebral space on their term equivalent scan, which are common imaging findings in preterm infants at term equivalent age. Their postnatal clinical courses were similar in terms of their respiratory requirements, exposure to sepsis, and number who had PDA. In addition, there were similar numbers of infants with IUGR and who received antenatal steroids in both groups. We have not, therefore, been able to identify any specific clinical risk factor associated with the development of punctate lesions. Our sample size is small and so larger studies may be required to identify clinical risk factors that are associated with punctate white matter lesions.

To date, there have been few studies assessing the impact of punctate WM lesions observed in the neonatal period on later neurodevelopmental performance (1,2,26). Cornette *et al.* (1) found that isolated punctate lesions, in the absence of major destructive lesions, were associated with favorable outcome at 30 mo of age. Similarly, we found no significant difference in developmental quotient scores, assessed between 18 and 36 mo of age, between preterm infants with punctate lesions and those who did not (2). Miller *et al.* described WM injury in a preterm population with early (32 wk) and near-term (37 wk) MR imaging. Their infants were classified as having minimal, moderate, and severe injury. They found that neurodevelopmental outcome at 18 mo of age was associated with the severity of injury (26). Follow-up data are not yet available on all of the infants reported here and will be the subject of further study. However, we would like to point out that although these lesions are associated with reduced FA in the corticospinal tracts, we have no evidence to show that isolated punctate lesions are generally associated with the development of CP.

In summary, in this study, punctate lesions were most commonly observed in the corona radiata/CSO and posterior periventricular WM and were associated with altered microstructure in the WM fibers of the corticospinal tract. Our results suggest that lesion load at term equivalent age adversely affects WM integrity. Follow-up studies are required to determine the functional consequence of punctate WM lesions.

Acknowledgments. We thank the families who took part in the study and our colleagues in the NICU and Children's Ambulatory Unit at Hammersmith Hospital.

REFERENCES

1. Cornette LG, Tanner SF, Ramenghi LA, Miall LS, Childs AM, Arthur RJ, Martinez D, Levene MI 2002 Magnetic resonance imaging of the infant brain: anatomical characteristics and clinical significance of punctate lesions. Arch Dis Child Fetal Neonatal Ed 86:F171–F177
2. Dyet LE, Kennea N, Counsell SJ, Maalouf EF, Ajayi-Obe M, Duggan PJ, Harrison M, Allsop JM, Hajnal J, Herlihy AH, Edwards B, Laroche S, Cowan FM, Rutherford MA, Edwards AD 2006 Natural history of brain lesions in extremely preterm infants studied with serial magnetic resonance imaging from birth and neurodevelopmental assessment. Pediatrics 118:536–548
3. Ramenghi LA, Fumagalli M, Righini A, Bassi L, Groppo M, Parazzini C, Bianchini E, Triulzi F, Mosca F 2007 Magnetic resonance imaging assessment of brain maturation in preterm neonates with punctate white matter lesions. Neuroradiology 49:161–167
4. Roelants-van Rijn AM, Groenendaal F, Beek FJ, Eken P, van Haastert IC, de Vries LS 2001 Parenchymal brain injury in the preterm infant: comparison of cranial ultrasound, MRI and neurodevelopmental outcome. Neuropediatrics 32:80–89
5. Le Bihan D, Breton E, Lallemand D, Grenier P, Cabanis E, Laval-Jeantet M 1986 MR imaging of intravoxel incoherent motions: application to diffusion and perfusion in neurologic disorders. Radiology 161:401–407
6. Moseley ME, Cohen Y, Kucharczyk J, Mintorovitch J, Asgari HS, Wendland MF, Tsuruda J, Norman D 1990 Diffusion-weighted MR imaging of anisotropic water diffusion in cat central nervous system. Radiology 176:439–445
7. Pierpaoli C, Basser PJ 1996 Toward a quantitative assessment of diffusion anisotropy. Magn Reson Med 36:893–906
8. Anjari M, Srinivasan L, Allsop JM, Hajnal JV, Rutherford MA, Edwards AD, Counsell SJ 2007 Diffusion tensor imaging with tract-based spatial statistics reveals local white matter abnormalities in preterm infants. Neuroimage 35:1021–1027
9. Counsell SJ, Shen Y, Boardman JP, Larkman DJ, Kapellou O, Ward P, Allsop JM, Cowan FM, Hajnal JV, Edwards AD, Rutherford MA 2006 Axial and radial diffusivity in preterm infants who have diffuse white matter changes on magnetic resonance imaging at term-equivalent age. Pediatrics 117:376–386
10. Hüppi PS, Maier SE, Peled S, Zientara GP, Barnes PD, Jolesz FA, Volpe JJ 1998 Microstructural development of human newborn cerebral white matter assessed in vivo by diffusion tensor magnetic resonance imaging. Pediatr Res 44:584–590
11. Neil JJ, Shiran SI, McKinstry RC, Schefft GL, Snyder AZ, Almli CR, Akbudak E, Aronovitz JA, Miller JP, Lee BC, Conturo TE 1998 Normal brain in human newborns: apparent diffusion coefficient and diffusion anisotropy measured by using diffusion tensor MR imaging. Radiology 209:57–66
12. Counsell SJ, Allsop JM, Harrison MC, Larkman DJ, Kennea NL, Kapellou O, Cowan FM, Hajnal JV, Edwards AD, Rutherford MA 2003 Diffusion-weighted imaging of the brain in preterm infants with focal and diffuse white matter abnormality. Pediatrics 112:1–7
13. Hüppi PS, Murphy B, Maier SE, Zientara GP, Inder TE, Barnes PD, Kikinis R, Jolesz FA, Volpe JJ 2001 Microstructural brain development after perinatal cerebral white matter injury assessed by diffusion tensor magnetic resonance imaging. Pediatrics 107:455–460
14. Smith SM, Jenkinson M, Johansen-Berg H, Rueckert D, Nichols TE, Mackay CE, Watkins KE, Ciccarelli O, Cader MZ, Matthews PM, Behrens TE 2006 Tract-based spatial statistics: voxelwise analysis of multi-subject diffusion data. Neuroimage 31:1487–1505
15. Behrens TE, Johansen-Berg H, Woolrich MW, Smith SM, Wheeler-Kingshott CA, Boulby PA, Barker GJ, Sillery EL, Sheehan K, Ciccarelli O, Thompson AJ, Brady JM, Matthews PM 2003 Non-invasive mapping of connections between human thalamus and cortex using diffusion imaging. Nat Neurosci 6:750–757
16. Bassi L, Ricci D, Volzone A, Allsop JM, Srinivasan L, Pai A, Ribes C, Ramenghi LA, Mercuri E, Mosca F, Edwards AD, Cowan FM, Rutherford MA, Counsell SJ 2008 Probabilistic diffusion tractography of the optic radiations and visual function in preterm infants at term equivalent age. Brain 131:573–582
17. Smith SM, Jenkinson M, Woolrich MW, Beckmann CF, Behrens TE, Johansen-Berg H, Bannister PR, De Luca M, Drobnjak I, Flitney DE, Niazy RK, Saunders J, Vickers J, Zhang Y, De Stefano N, Brady JM, Matthews PM 2004 Advances in functional and structural MR image analysis and implementation as FSL. Neuroimage 23:S208–S219
18. Ball G, Counsell SJ, Anjari M, Merchant N, Arichi T, Doria V, Rutherford MA, Edwards AD, Rueckert D, Boardman JP 2010 An optimised tract-based spatial

statistics protocol for neonates: applications to prematurity and chronic lung disease. Neuroimage 53:94–102

19. Wakana S, Caprihan A, Panzenboeck MM, Fallon JH, Perry M, Gollub RL, Hua K, Zhang J, Jiang H, Dubey P, Blitz A, van Zijl P, Mori S 2007 Reproducibility of quantitative tractography methods applied to cerebral white matter. Neuroimage 36:630–644
20. Johansen-Berg HB, Behrens TE 2009 Diffusion MRI: From Quantitative Measurement to In-Vivo Neuroanatomy. Elsevier, London, pp 333–353
21. Fan GG, Yu B, Quan SM, Sun BH, Guo QY 2006 Potential of diffusion tensor MRI in the assessment of periventricular leukomalacia. Clin Radiol 61:358–364
22. Hoon AH Jr, Lawrie WT Jr, Melhem ER, Reinhardt EM, Van Zijl PC, Solaiyappan M, Jiang H, Johnston MV, Mori S 2002 Diffusion tensor imaging of periventricular leukomalacia shows affected sensory cortex white matter pathways. Neurology 59:752–756
23. Nagae LM, Hoon AH Jr, Stashinko E, Lin D, Zhang W, Levey E, Wakana S, Jiang H, Leite CC, Lucato LT, van Zijl PC, Johnston MV, Mori S 2007 Diffusion tensor imaging in children with periventricular leukomalacia: variability of injuries to white matter tracts. AJNR Am J Neuroradiol 28:1213–1222
24. Thomas B, Eyssen M, Peeters R, Molenaers G, Van Hecke P, De Cock P, Sunaert S 2005 Quantitative diffusion tensor imaging in cerebral palsy due to periventricular white matter injury. Brain 128:2562–2577
25. Rutherford MA, Supramaniam V, Ederies A, Chew A, Bassi L, Groppo M, Anjari M, Counsell S, Ramenghi LA 2010 Magnetic resonance imaging of white matter diseases of prematurity. Neuroradiology 52:505–521
26. Miller SP, Ferriero DM, Leonard C, Piecuch R, Glidden DV, Partridge JC, Perez M, Mukherjee P, Vigneron DB, Barkovich AJ 2005 Early brain injury in premature newborns detected with magnetic resonance imaging is associated with adverse early neurodevelopmental outcome. J Pediatr 147:609–616